Decoding Gemini Planet Imager (GPI) Observations of Debris Disks

Christine H. Chen (STScI, JHU)

on behalf of

Johan Mazoyer (JHU), Charles Poteet (STScI), Gaspard Duchene (UC Berkeley), Justin Hom (ASU), Jenny Patience (ASU), Bin Ren (JHU), Laurent Pueyo (STScI), Pauline Arriaga (UCLA), Michael Fitzgerald (UCLA), Max Millar-Blanchaer (Caltech/JPL)

Meteoritic Constraints on Planet Formation

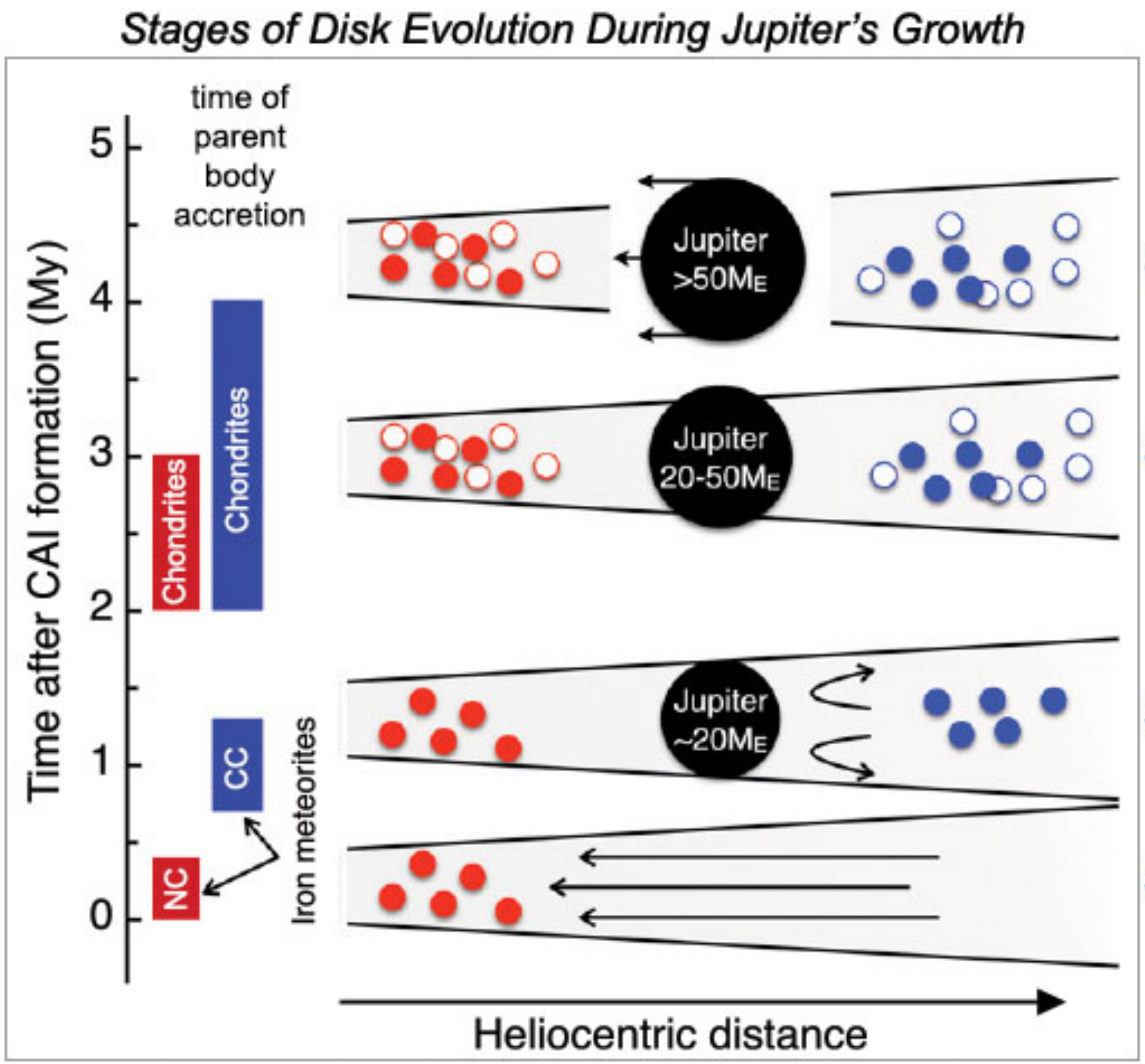

(From Kruijer, T. S., *et al.*, 2017, *PNAS*, doi: 10.1073/pnas.1704461114.)

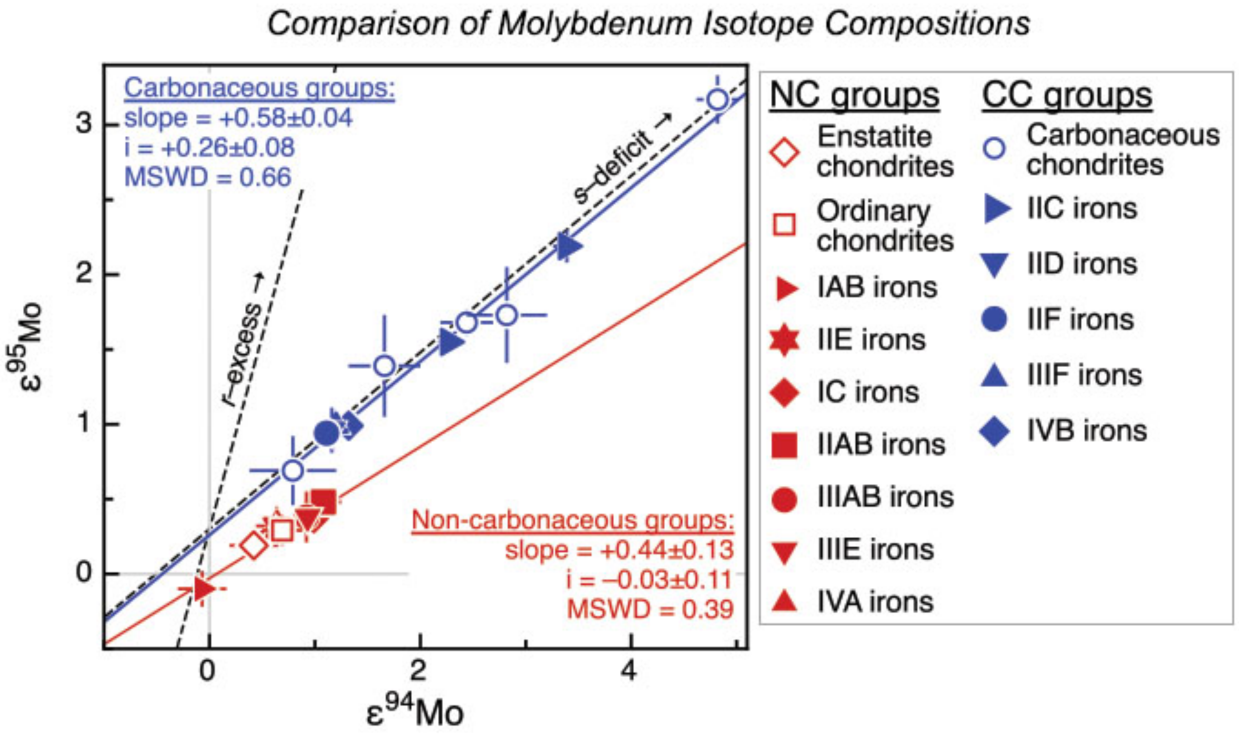

- Molybdenum and Tungsten isotope ratios suggest that Solar System bodies derive from two genetically distinct nebular reservoirs
- The formation of Jupiter's core at an age of 1 Myr naturally explains the existence of two reservoirs

Debris Disk Dust Constraints

Spectral Energy Distribution

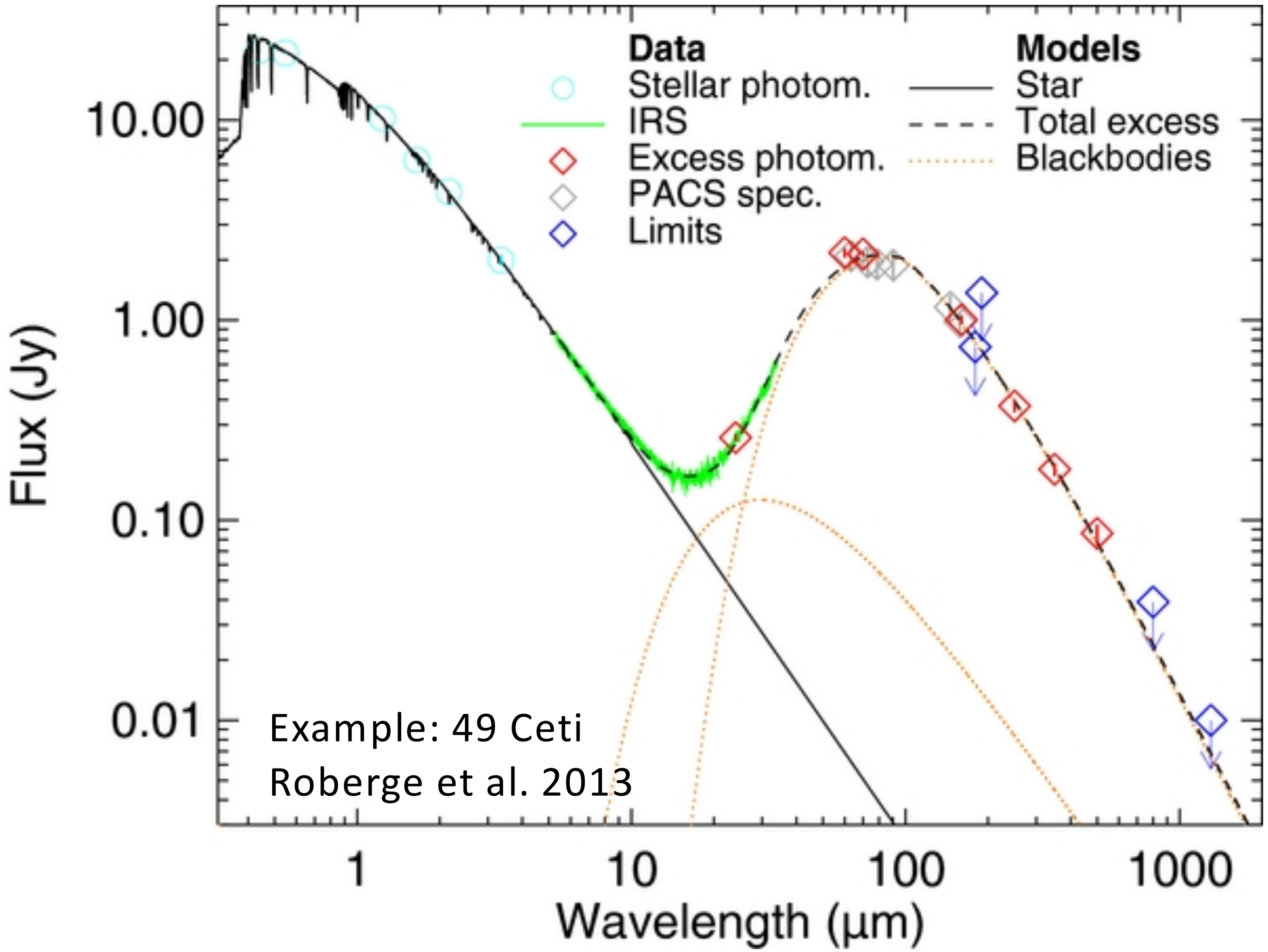

Example: 49 Ceti
Roberge et al. 2013

Scattered Light Images

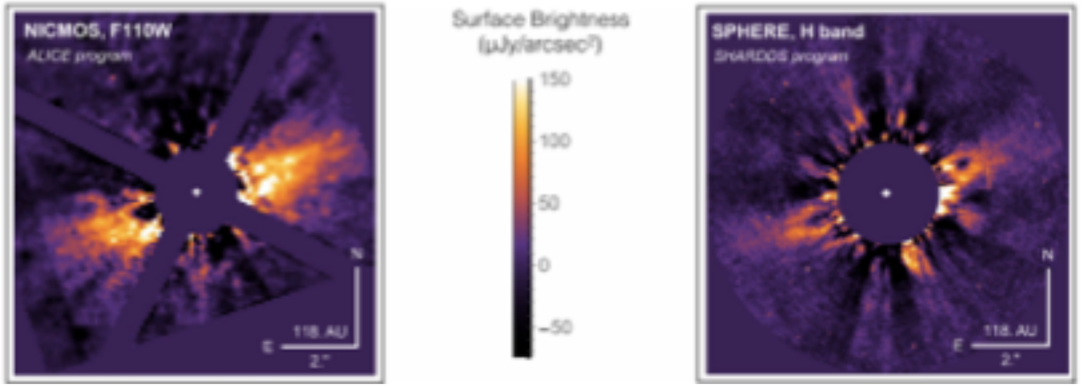

Choquet et al. 2017

Thermal Emission Images

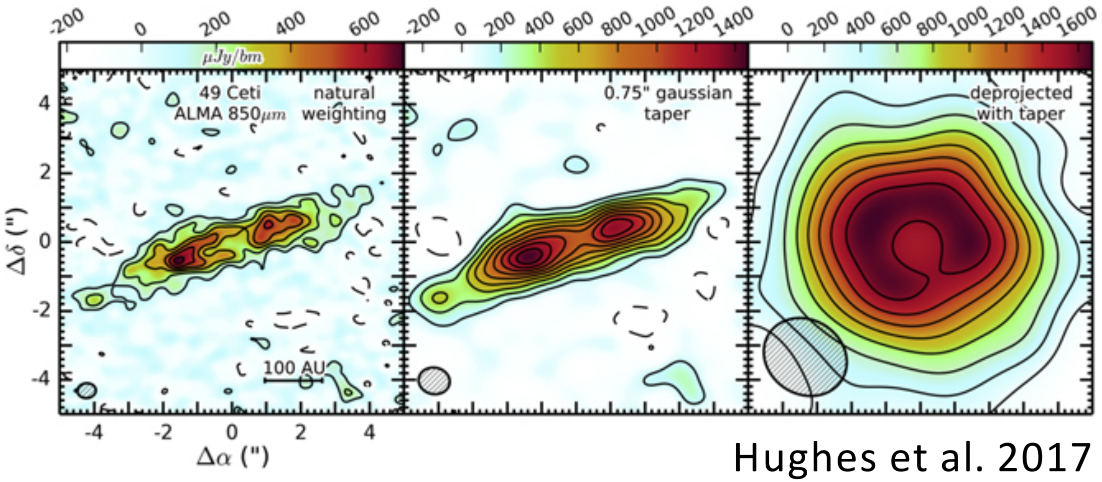

Hughes et al. 2017

GPI Capabilities

Polarimetry

J-coron: 1.12 – 1.35 µm
(IWA = 92 mas)

K1-coron: 1.9 – 2.19 µm
(IWA = 153 mas)

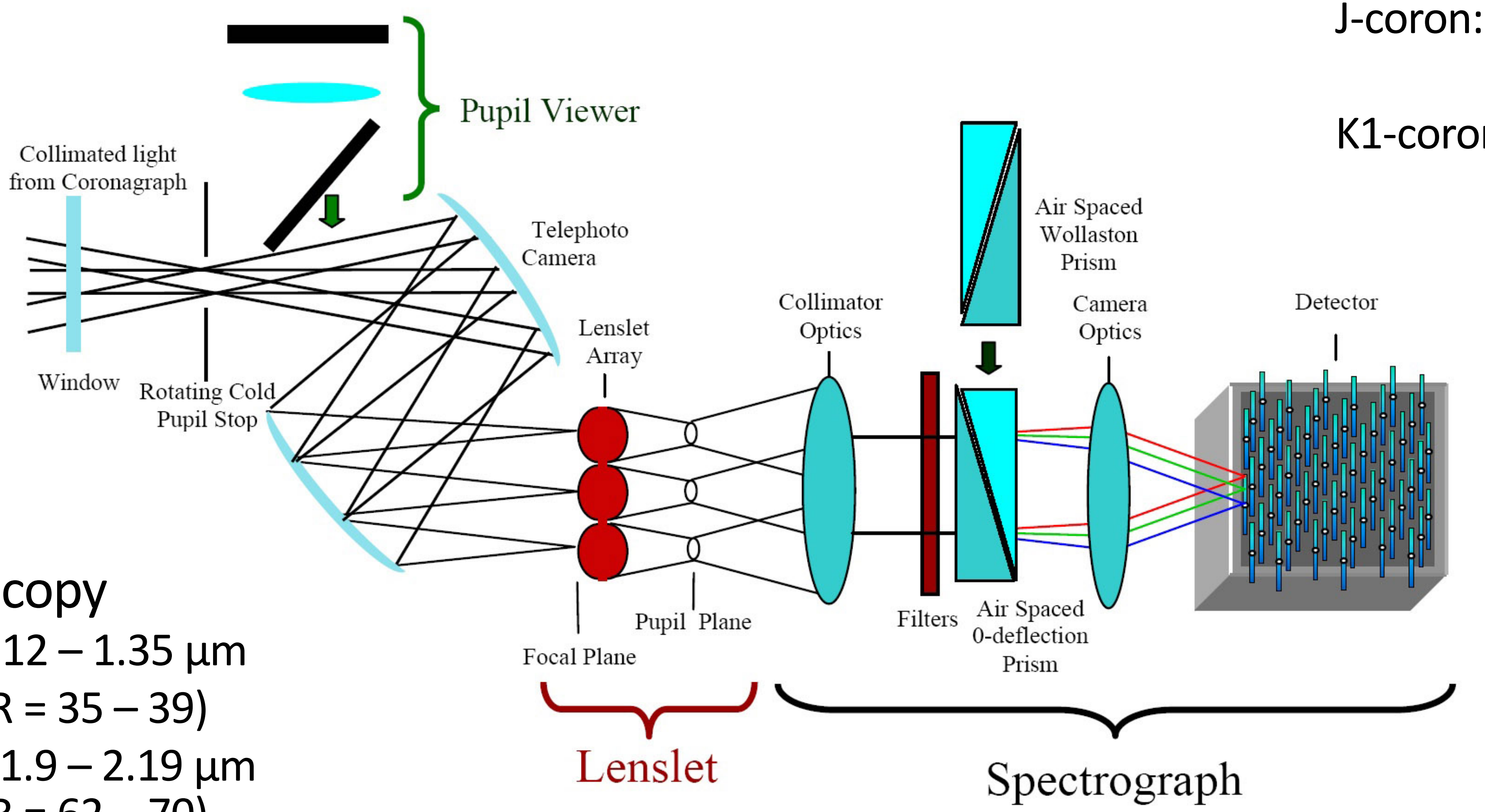

Spectroscopy

J-coron: 1.12 – 1.35 µm
(R = 35 – 39)

K1-coron: 1.9 – 2.19 µm
(R = 62 – 70)

Thibault 2010

Scattered Light Observables

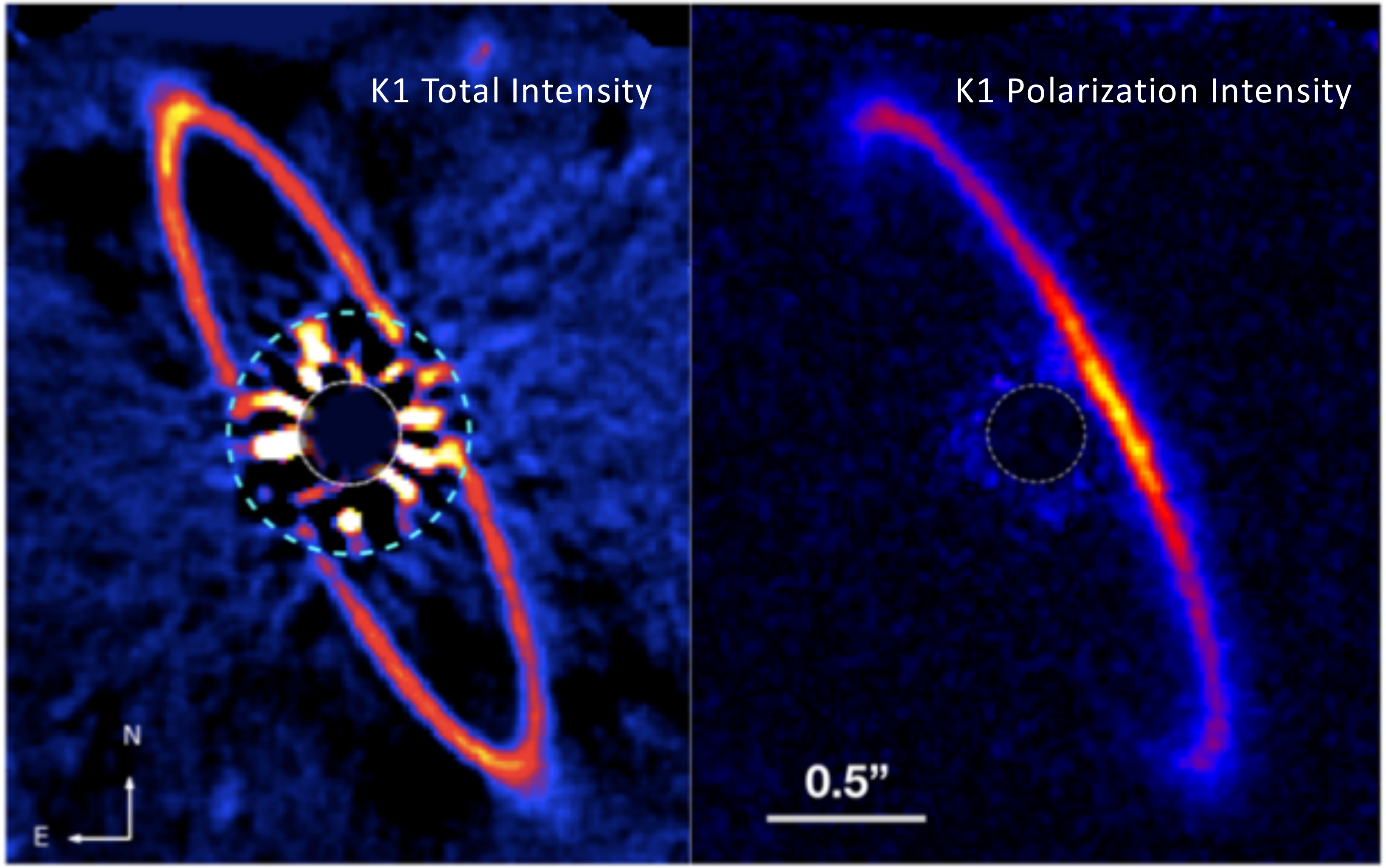

- Disk geometry
- Total intensity phase function
- Polarization fraction phase function
- Reflected light spectrum
- Polarization fraction color

Perrin et al. (2015)

GPI Observing Sequences

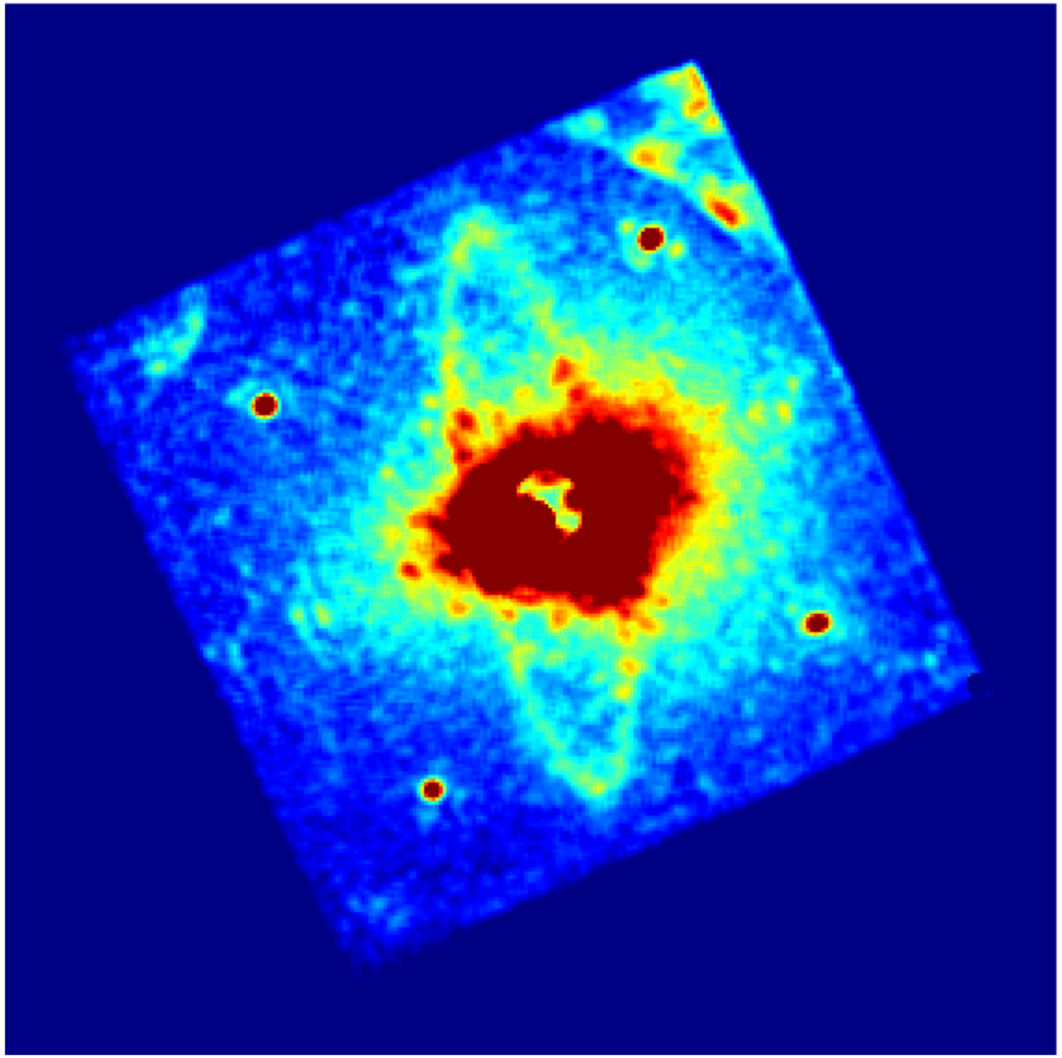

- To facilitate Angular Differential Imaging (ADI), the source is allowed to rotate with respect to the instrument field of view and exposures are taken every 60 – 90 sec
- The maximum rotation rate occurs near transit.
- Disk may fall on PSF structures (e.g. satellite spots) during an observational sequence. The photon noise from the satellite spots is significantly higher than the disk surface brightness. Thus, these frames can not be incorporated into the scientific analysis

Data Challenges

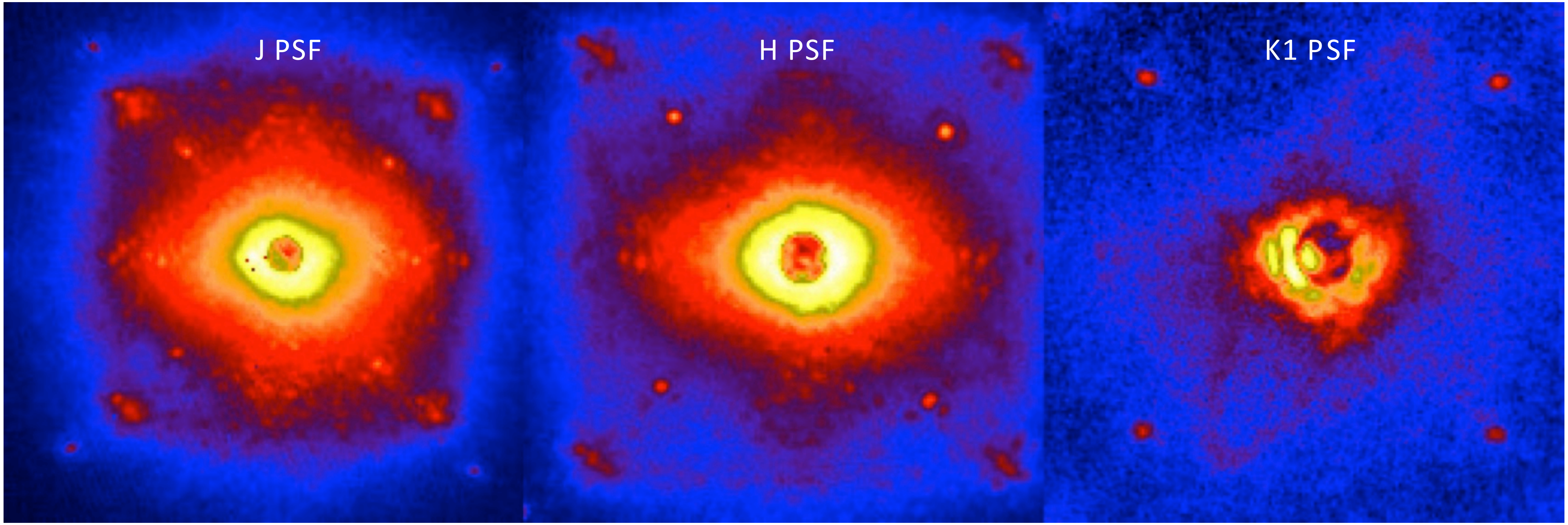

- Complicated Point Spread Function
- Lower Strehl Ratio for Shorter Wavelength filters
- Changing Seeing Conditions

PSF Estimation and Subtraction

- **Mask and Interpolate** – For observations of bright disks, mask disk and interpolate PSF under the mask
- **RDI-NMF** – For H-band (with GPIES reference library), construct PSF from reference observations using NMF
- **RDI-KLIP** – For H-band (with GPIES reference library), construct PSF from reference observations using KLIP
- **ADI-KLIP** – Construct PSF from observational sequence using KLIP

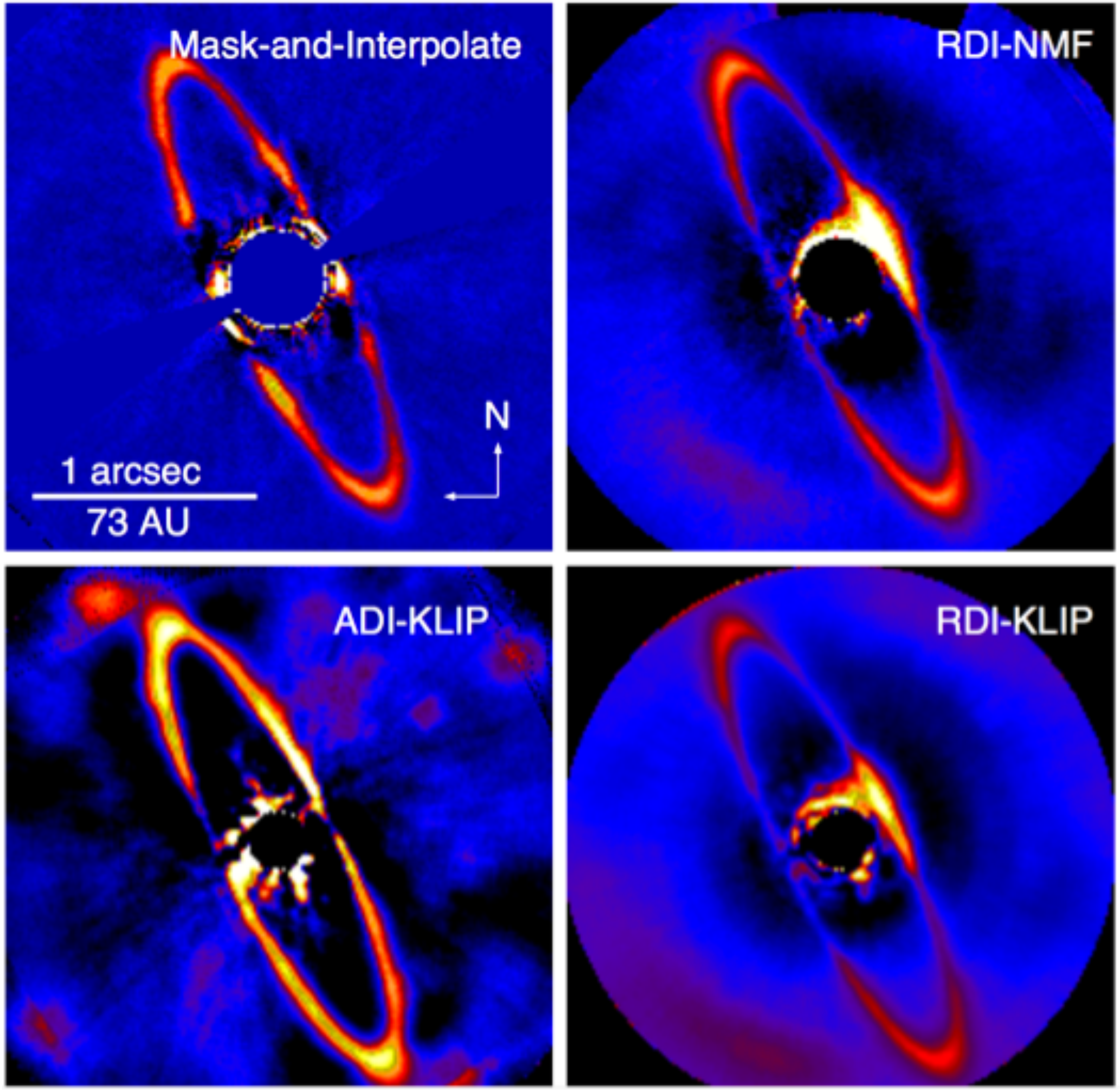

Disk Geometry

Projected

a' = 1070 mas

e' = 0.971

PA' = 206.5

ΔRA = 7 mas

ΔDec = -10 mas

Deprojected

a = 1070 mas

e = 0.02

i = 76.1

ω = unconstrained

Ω = 26.5

- Exclusion angle increases from RDI-KLIP to RDI-NMF to ADI-KLIP to Mask-and-Interpolate
- Impact on measured geometry is the largest for ADI-KLIP

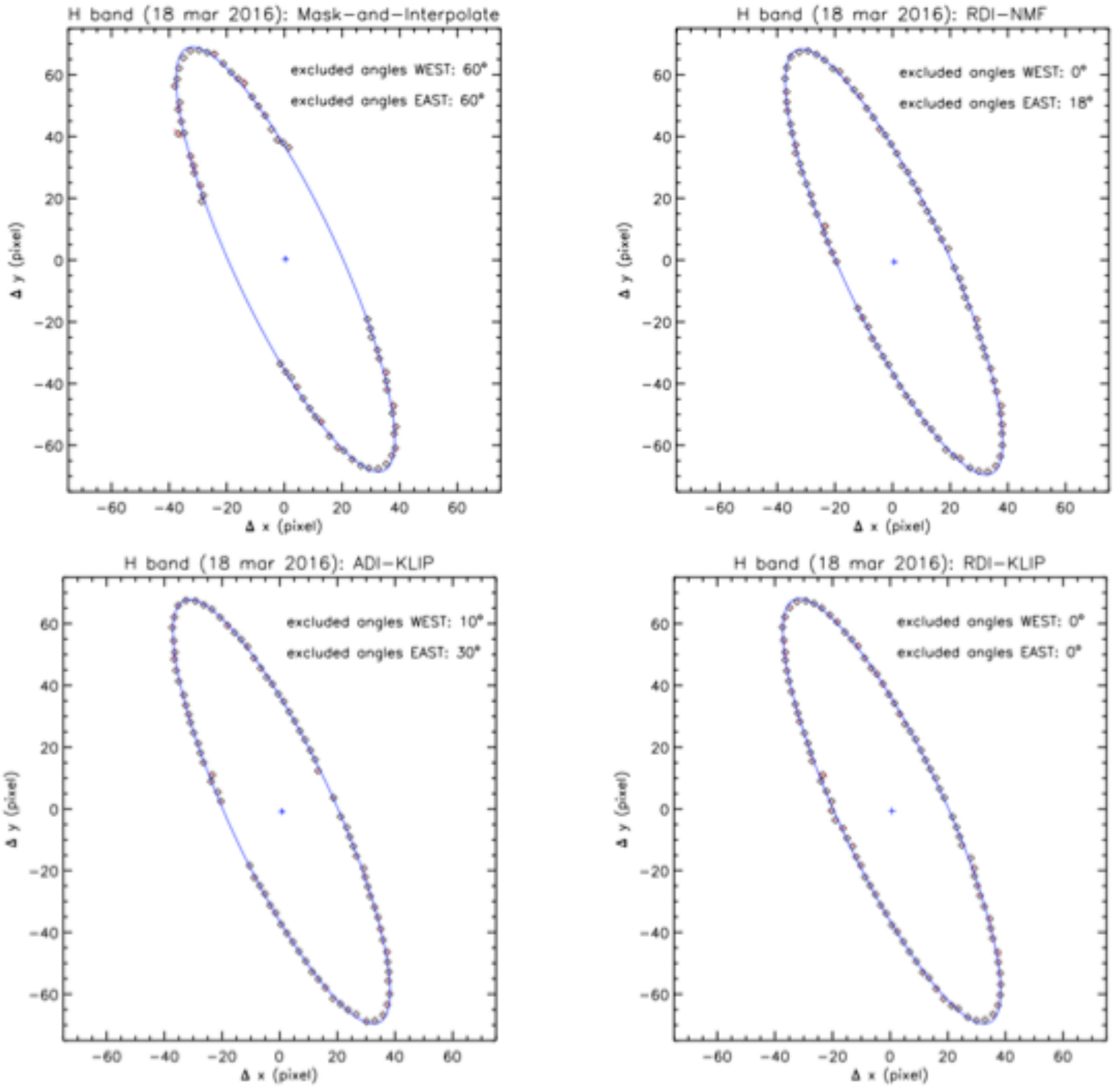

Pericenter and Apocenter Glow

- GPI HR 4796 observations indicate that the NE ansa is ~10% brighter than the SW. In reflected light, the pericenter is expected to be $((1+e)/(1-e))^2$ brighter than the apocenter.
- In mid-infrared thermal emission, the pericenter is expected to be ~5% brighter than the apocenter for e ~ 0.02
- In sub-millimeter emission, the apocenter is expected to be (1+e)/e brighter than the pericenter. ALMA observations do not currently possess sufficient SNR to detect apocenter glow.

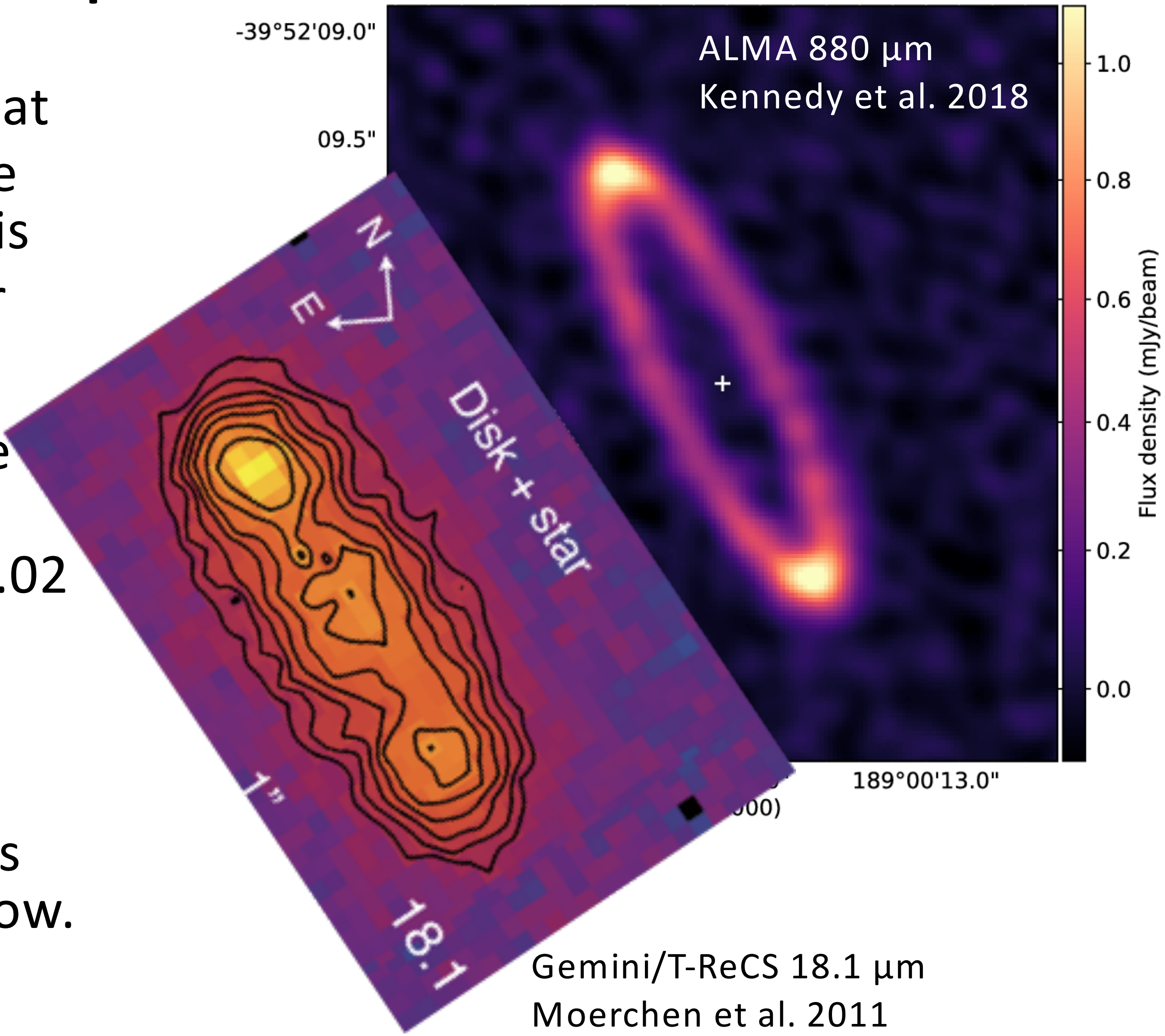

Gemini/T-ReCS 18.1 μm
Moerchen et al. 2011

Isotropic Phase Function

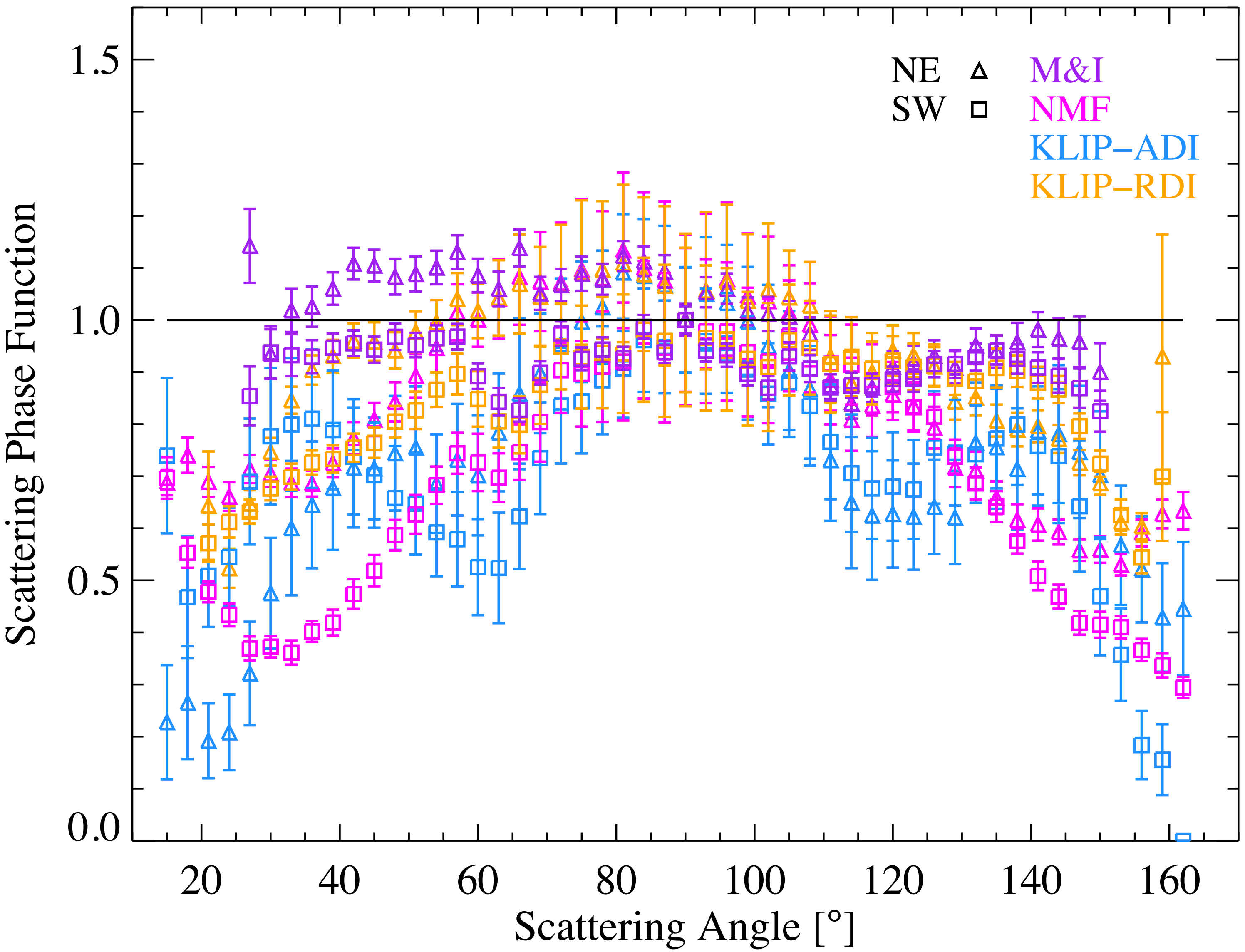

- Mask-and-Interpolate alters the scattering phase function the least with little over subtraction over a broad range of scattering angles (40-145)
- RDI-NMF and RDI-KLIP produce more over-subtraction at a larger range of angles near forward and backward scattering
- ADI-KLIP generates additional wavy structure beyond the over-subtraction at forward and backward scattering

HR 4796A H-Band Phase Function

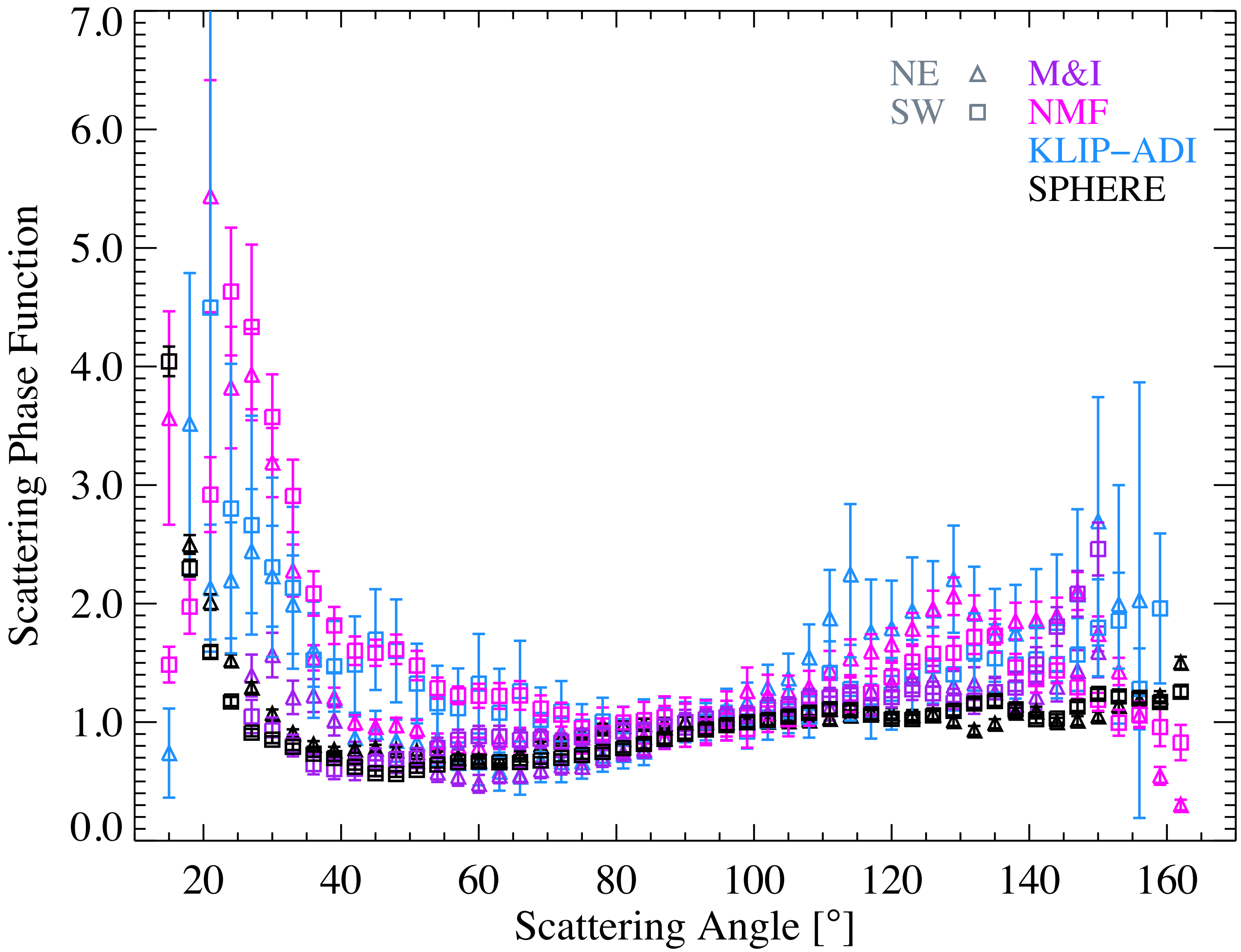

Once the HR 4796A phase function is corrected using the extracted isotropic scattering phase function

- Mask-and-Interpolate provides the most consistent result with SPHERE
- Other techniques indicate more forward and backward scattering behavior that is likely the result of mismatches in brightness between the observed disk and injected disk

Constraints from Forward Scattering Grains

- Mie and/or DHS grains are unable to reproduce the full behavior of the measured phase function
- Fits to the phase function at φ < 45° suggest the presence of a steep power law distribution ν = -5.5 with a minimum grain size s_{min} = 17.8 µm, similar to the expected blow out size
- Fits to the backscattering are consistent with large regolith particles described by Hapke theory

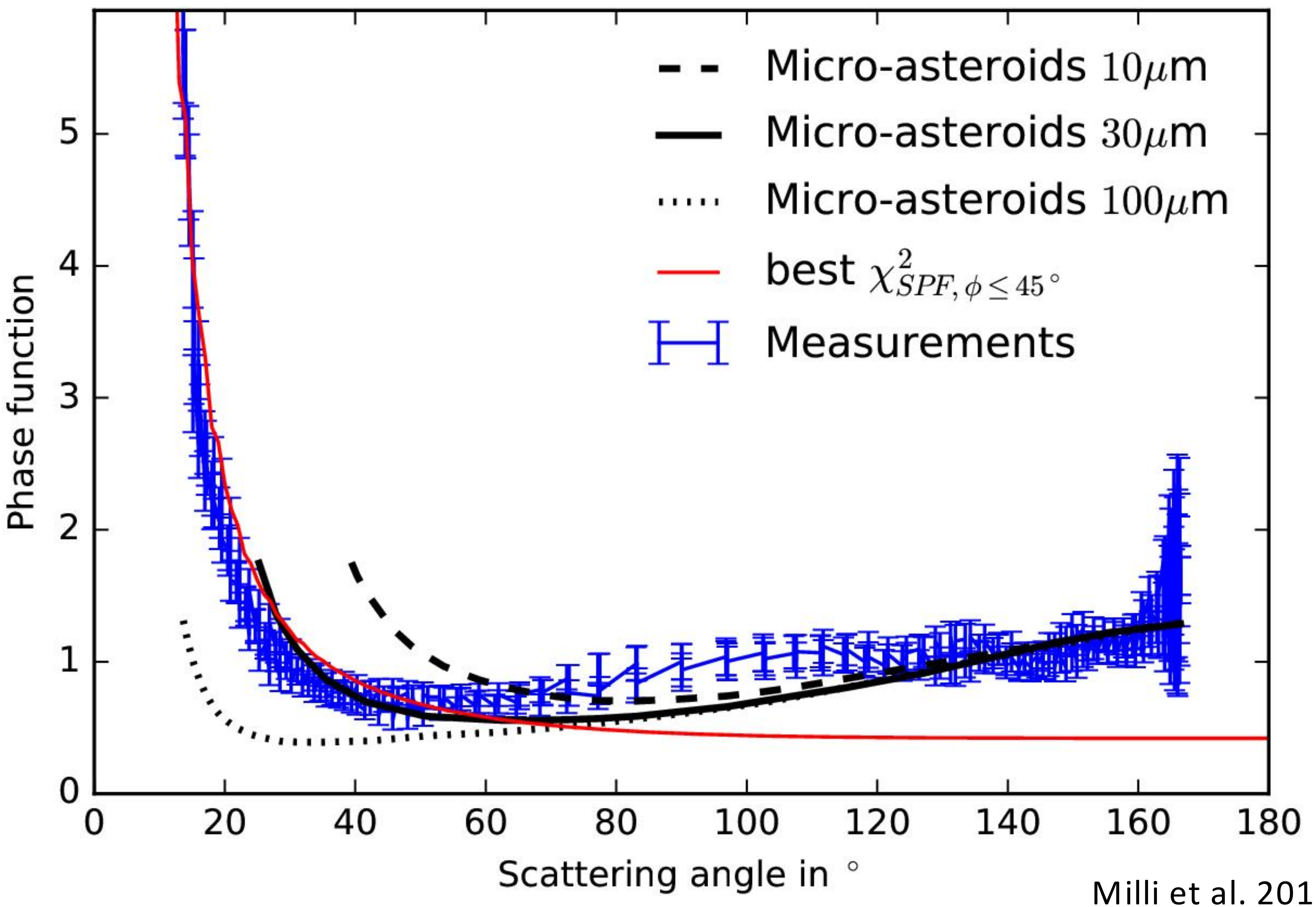

Milli et al. 2017

HR 4796A Phase Function Color

The ratio of the HST STIS (visual) to GPI K1 scattering phase function indicates

- More visual light is scattered at intermediate scattering angles
- Future work is to better constrain the grain size from the color

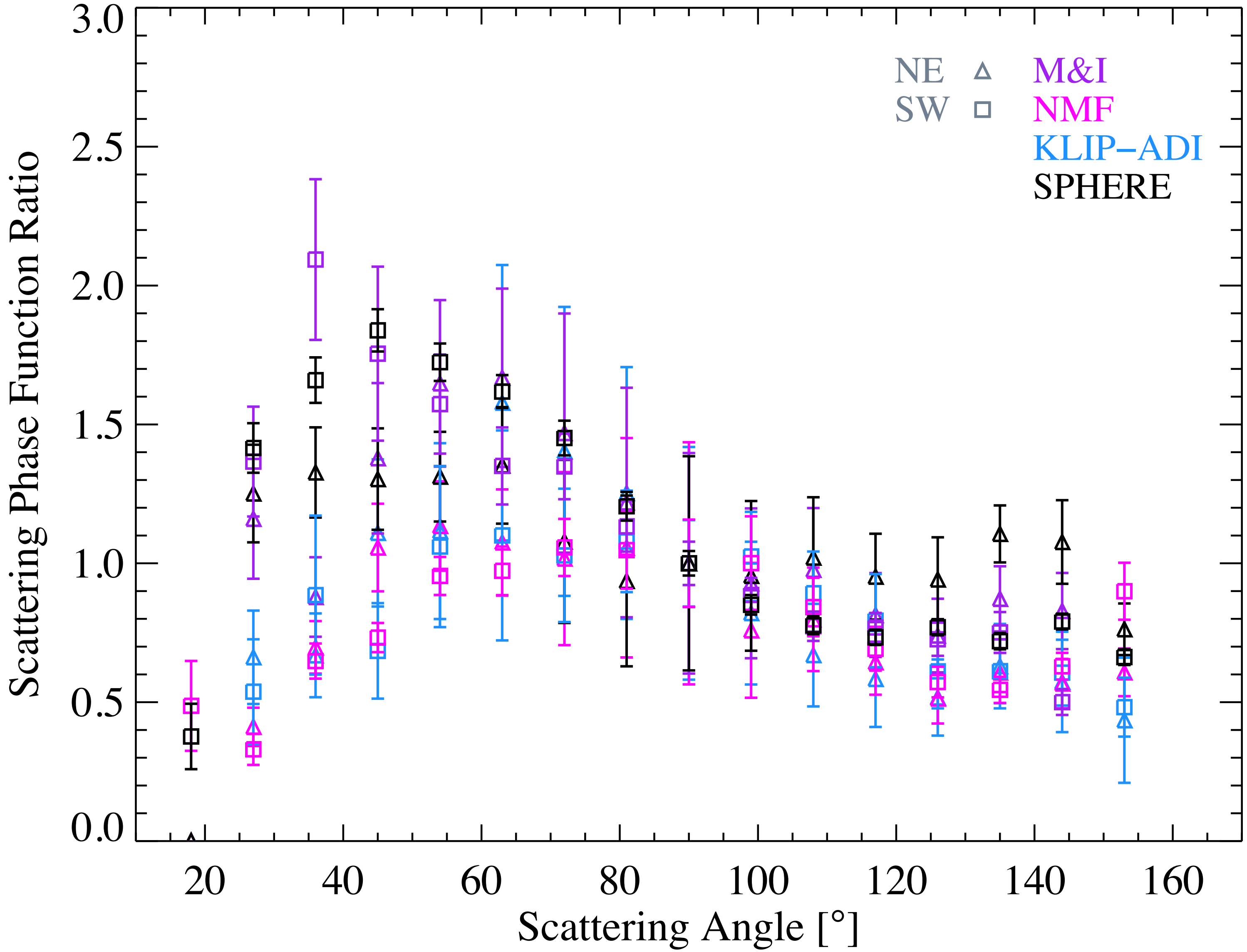

HR 4796A Polarization Fraction Phase Function

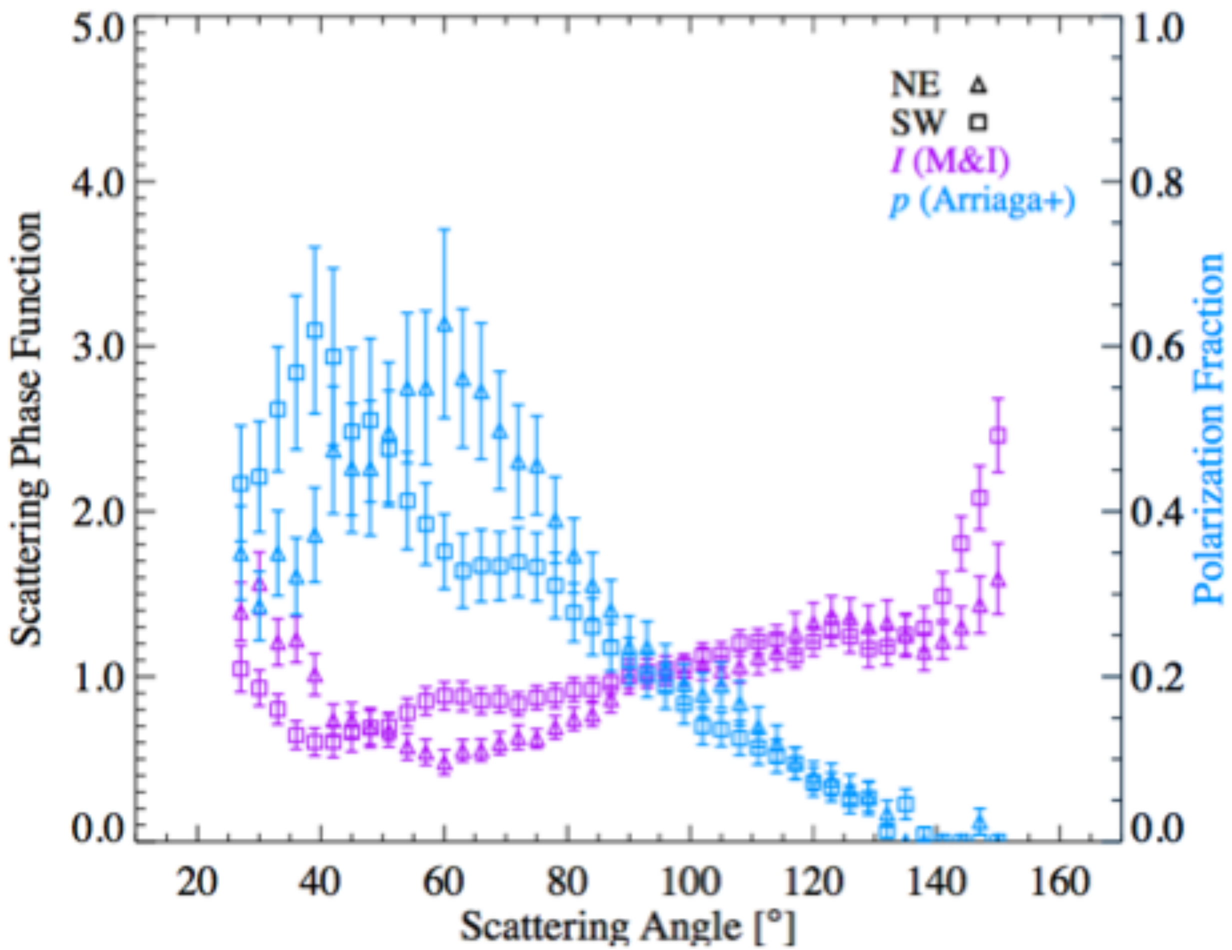

Consistent with preliminary K1 results reported by Perrin et al. (2015)

- Shows shift in peak polarization fraction at scattering angles <90°, consistent with the presence of large grains (Mie Theory)
- Future work: explore the color dependence of the polarization fraction phase function and dependence on grain shape

HR 4796A Reflected Light Spectrum

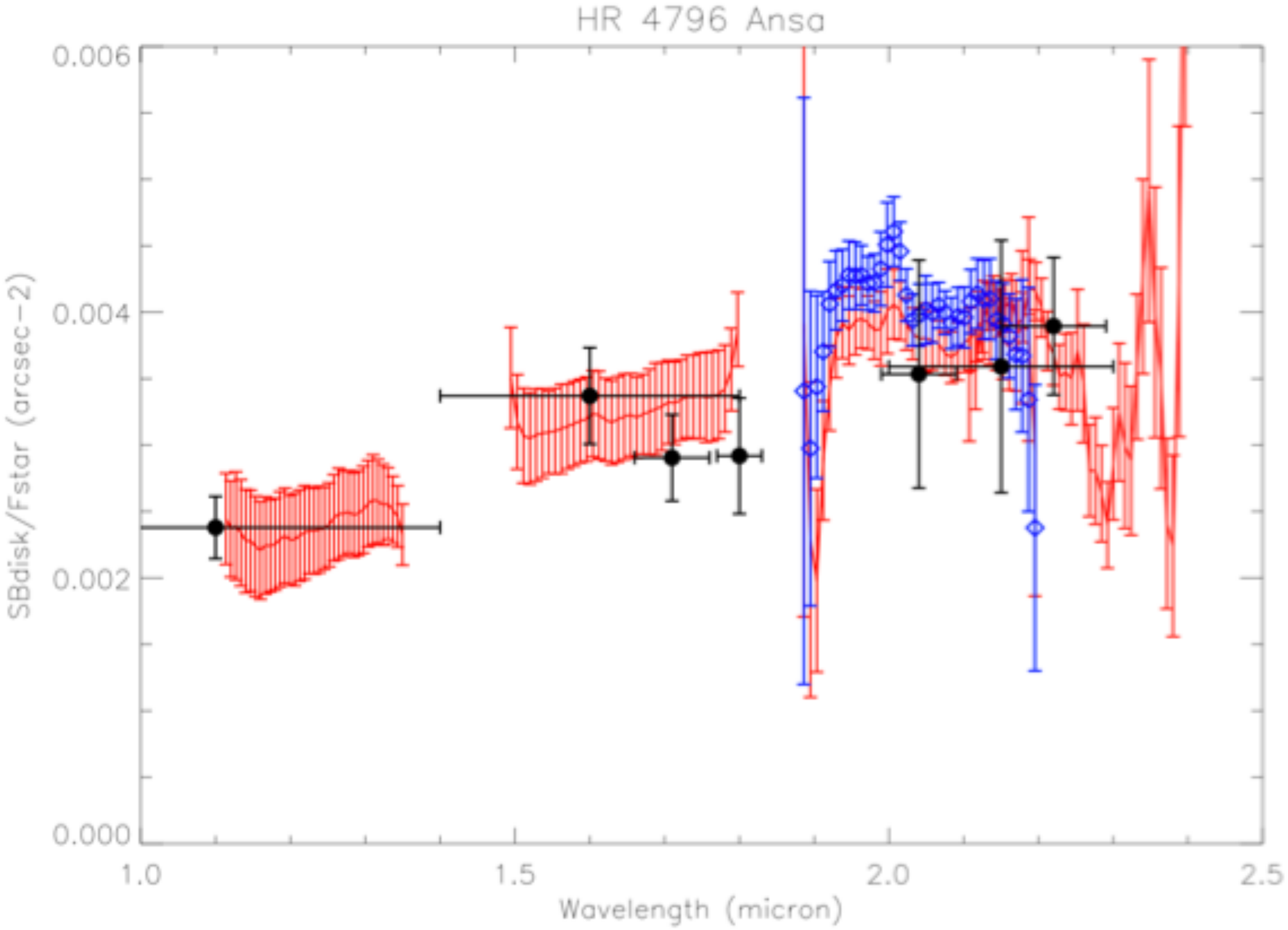

- Falling behavior beyond 2.2 μm is like the result of the reduced throughput of the instrument coupled with the higher background
- Shape of the scattered light SED is consistent with previous observations
- No obvious solid state features are detected (as would be expected from H_2O and other ices)

LLP Observations Thus Far

Table 1. Debris Characterization LLP 2015B-2017B Observations

Name	Sp Type	Dist (pc)	Age (Myr)	D (AU)	i	GPI Request	New GPI Observations
49 Cet	A1V	59	40	65-250	73°		Pol: J, K_1
HD 15115	F2	45	12	31-315	90°	IFS: Y, J, K_1	IFS: J, H, K_1 Pol: J, H
HD 30447	F3V	80	10-40	60-200			Pol: J, K_1
HD 32297	A0V	112	30	50-1680	90°	IFS: Y, J, K_1 Pol: Y, J, K_1	IFS: J, H, K_1, K_2 Pol: J, K_1
HD 35650	K6V	18	50-200	49-68	89°		Pol: K_1
HD 35841	F3V	96	30	50-1680	90°	IFS: Y,J, K_1 Pol: Y, J, K_1	IFS: J, K_1
HD 36546	B8	113	~10	50-1200	90°	IFS: H; Pol: H	IFS: H; Pol: H
β Pictoris	A5V	19	30	100-1300	90°	Pol: J, K_1	IFS: Y, J
HD 61005	G8V	18	45	62	85°	IFS: Y, K_1 Pol: Y, J, K_1	IFS: J, K_1 Pol: J
HD 106906	F5V	92	16	50-500	85°		IFS: J, K_1 Pol: J, K_1
HD 110058	A0V	107	17	20-65	90°		IFS: J, K_1 Pol: J, K_1
HD 111520	F5-6V	108	17	35-650	85°	IFS: Y, J, K_1 Pol: Y, J, K_1	IFS: J, K_1 Pol: J, K_1
HD 114082	F3V	85	17	25-30	83°		Pol: K_1
HD 115600	F2IV/V	110	17	38-55	80°		IFS: J, K_1 Pol: J, K_1
HD 129590	G1V	133	16	60-70	75°		IFS: J Pol: K_1
HD 146897	F2V	123	11	25-250	90°	IFS: Y,J, K_1 Pol: Y, J, K_1	IFS: J, K_1 Pol: J
HD 157587	F5-F6	109	~3000	50-650	90°	IFS: Y,J, K_1 Pol: Y, J, K_1	IFS: K_1 Pol: J, K_1

Note: The observations listed in red were begun but not completed with the target disk SNR.

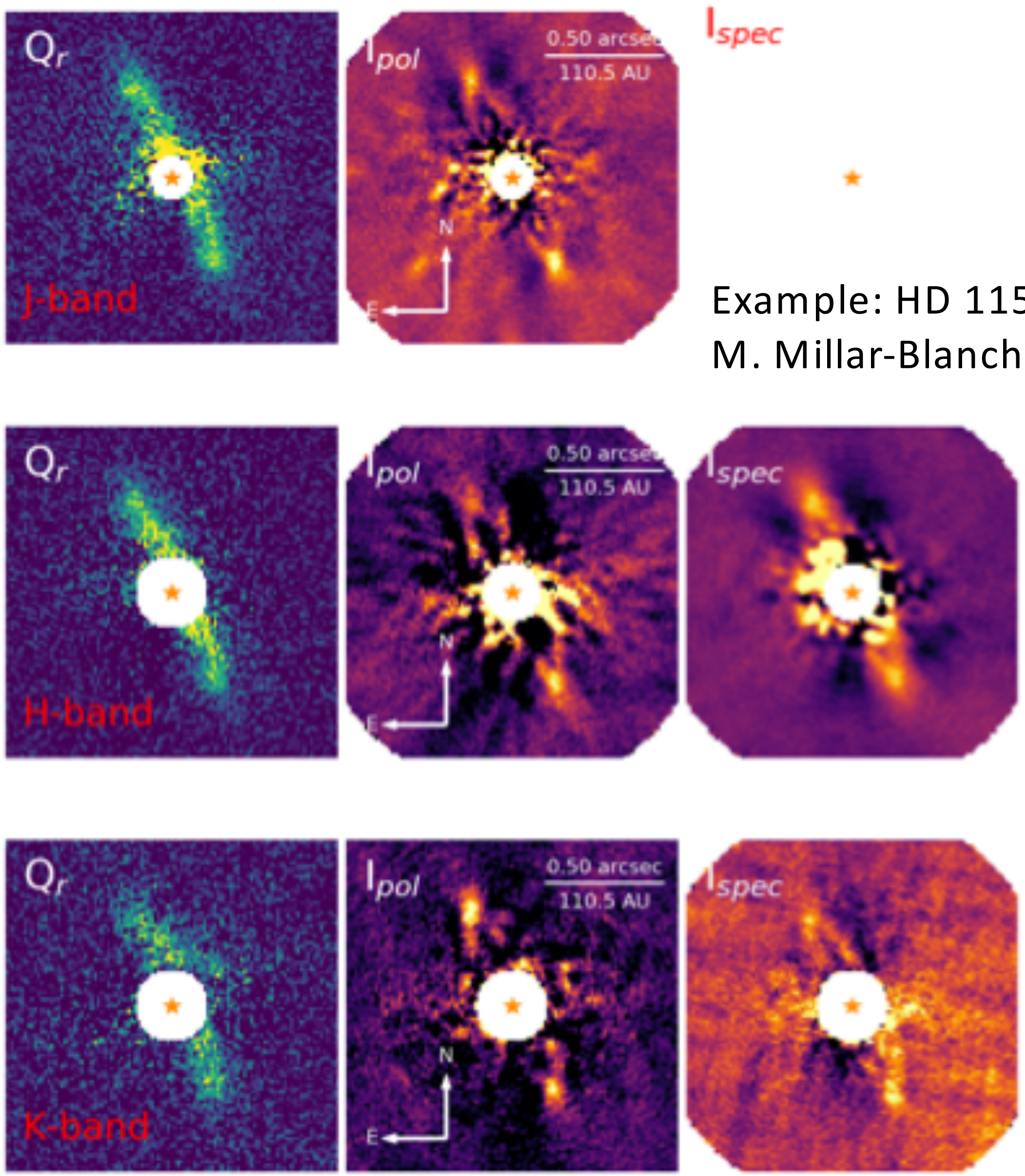

Example: HD 115600
M. Millar-Blanchaer

Conclusions and Future Work

- Basic tools are in place to extract geometric parameters, total intensity and polarization fraction phase functions, and reflected light spectra and polarization intensity colors
- Sources possess a wide variety of inclinations and surface brightnesses. Thus, addressing each source requires tailored analysis to understand the impact of PSF subtraction and ensure that underlying disk observables are extracted accurately.
- Effort is ramping up to interpret the observables. Plan to use MCFost radiative transfer code to explore scattering and thermal emission properties of ensembles of aggregates using Mie and Distribution of Hollow Spheres (DHS)